Resonance ionization spectroscopy and analysis on even-parity states of Pb I

Shuichi Hasegawa and Atsuyuki Suzuki
Department of Quantum Engineering and Systems Science, The University of Tokyo, 7-3-1 Hongo, Bunkyo-ku, Tokyo 113, Japan
(Received 12 October 1995)

Two-color resonance ionization spectroscopies of Pb, even parity, $J=0$, 1, and 2 levels were performed and their term values were analyzed with multichannel quantum defect theory. We have observed $6pnp(\frac{1}{2},\frac{1}{2})_0$ $(28\leqslant n\leqslant 50)$, $6p7p(\frac{3}{2},\frac{3}{2})_0$, $6pnp(\frac{1}{2},\frac{3}{2})_1$ $(14\leqslant n\leqslant 27)$, $6pnp(\frac{1}{2},\frac{3}{2})_2$ $(42\leqslant n\leqslant 54)$, and $6pnf\ ^1_2[^5_2]_2$ $(28\leqslant n\leqslant 51)$. Fitting multichannel quantum defect theory (MQDT) parameters to minimize deviation between the observed and theoretical energy values, we determined quantum defects μ_α and unitary matrix elements $U_{i\alpha}$ for $J=0$, 1, and 2 even-parity levels. Calculating theoretical energy values and determining their assignment with MQDT, we assigned observed levels and predicted unobserved levels and perturbers. Admixture coefficients for perturbing levels of $J=0$, 1, and 2 were calculated in order to ensure their assignments.

PACS number(s): 32.20.−r, 31.15.Ct, 32.80.Rm

I. INTRODUCTION

Resonance ionization spectroscopy (RIS) of atoms has become extensive and successful for the past two decades. Using the multistep resonance method, enabled excitation, with almost unity, of any state of interest; for example, high-lying states and high-angular-momentum states that were difficult to investigate with other spectroscopic methods. This multistep has also provided high-resolution energy values of excited states because an energy value of an intermediate excited state can be determined by the wavelength of the exciting laser. RIS, therefore, has revealed characteristics of high-lying Rydberg states.

On the other hand, theoretical methods for describing high-lying states have also been developed. One of them is multichannel quantum defect theory (MQDT), which was first derived by Seaton [1,2] and extended by Fano and coworkers [3–8]. Reference [3] suggested an empirical method of Seaton's MQDT to show perturbed series by a graphical method using periodicity, and demonstrated it with rare-gas and Ba spectra. The figure, which is called the ''Lu-Fano plot'' after their work, represents perturbations of different configurations. In Ref. [4], application of Seaton's MQDT was performed to the spectra of H_2 high-lying states under schematic conditions. References [5, 6] analyzed rare-gas spectra with MQDT. The references described in detail the practical approach of the theory to rare-gas spectra.

One of the periodic groups that have two low-lying ionic core states is the carbon group, which is interesting from the point of view of MQDT. The ground-state configuration of the carbon group is $ns^2np^2\ ^3P_0$. The ground configuration of the ionic core is $ns^2np\ ^2P_{1/2}$. This means that the excited state of the ionic core near the first ionization limit is only $^2P_{3/2}$. Brown *et al.* made a series of absorption spectroscopy experiments of the carbon group with a rare-gas lamp and spectrograph, and applied MQDT to the electronic states of the carbon group [9–13]. Their experimental apparatus limited their investigation to odd-parity states because of dipole selection rules, since the ground electronic state is even parity.

The heaviest element of the carbon group is lead (Pb). The ground configuration of Pb I is $6s^26p^2\ ^3P_0$, and the ionic core (Pb II) is $6s^26p$, which splits into two levels, $^2P^o_{1/2}$ (lower ionization limit) and $^2P^o_{3/2}$ (upper ionization limit) in the LS coupling scheme. The early data before 1960 were summarized by Moore [14]. Garton and Wilson investigated odd-parity $6pns$ $(8\leqslant n\leqslant 32)$ and $6pnd$ $(6\leqslant n\leqslant 53)$ series with absorption spectroscopy [15]. Wood and Andrew observed the emission spectra of Pb and determined the low-lying states of even and odd parity [16]. Brown *et al.* reported absorption spectra between 1350 and 2041 Å and assigned $6pns$, $6pnd$, $J=0,1,2$, odd-parity series with MQDT [13]. They determined 59 819.57 and 73 900.64 cm^{-1} for the ionization limits of $6p\ ^2P^o_{1/2}$ and $6p\ ^2P^o_{3/2}$, respectively. The laser spectroscopy experiment of even parity has been performed recently by several groups. Young *et al.* used three-photon hybrid resonance spectroscopy to observe even-parity $6pnp(\frac{1}{2},\frac{1}{2})_0$, $(\frac{1}{2},\frac{3}{2})_1$, and $(\frac{1}{2},\frac{3}{2})_2$ series up to $n=23$, 20, and 48, respectively, and $6pnf\ ^1_2[^5_2]_2$ series to $n=26$ [17]. In three-photon hybrid resonances, excited states of atoms are prepared by the dissociation of the diatomic molecule because of two-photon absorption. The advantage of this method is to populate intermediate states of both even and odd parity. Ding *et al.* observed $6pnp(\frac{1}{2},\frac{1}{2})_0$, $10\leqslant n\leqslant 27$, $(\frac{1}{2},\frac{3}{2})_2$, $10\leqslant n\leqslant 41$, and $6pnf\ ^1_2[^5_2]_2$, $7\leqslant n\leqslant 27$ even-parity Rydberg states with two-photon RIS, and analyzed spectra with MQDT [18]. Ma *et al.* demonstrated a two-color RIS experiment of Pb to excite $6p(^3P^o_{1/2})7s\ ^3P^o_1$ as an intermediate state [19]. The spectroscopic data for even-parity Rydberg states of Pb, however, are much less complete so far. These data are important not only for atomic spectroscopy data but also for the applications using Pb.

Resonance ionization spectroscopy of Pb with mass spectrometry, which is called resonance ionization mass spectrometry, was applied to analyze multielement samples [20], and remove their isobaric interferences with bismuth [21]. These applications have been important in the fields of environmental pollution, age determination, and so on.

In this paper we will use two-color resonance ionization spectroscopy of Pb to excite $6p(^3P^o_{1/2})7s\ ^3P^o_1$ as an intermediate state to investigate even-parity $J=0$, 1, and 2 Rydberg series, and analyze the data with MQDT. The intermediate state of $6p(^3P^o_{1/2})7s\ ^3P^o_1$ was investigated with various spectroscopic methods in Refs. [14, 16, 22–25]. The

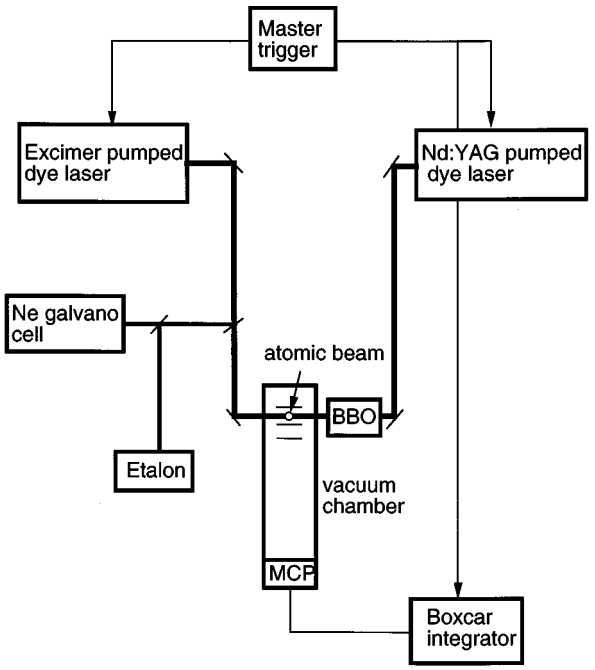

FIG. 1. Experimental setup.

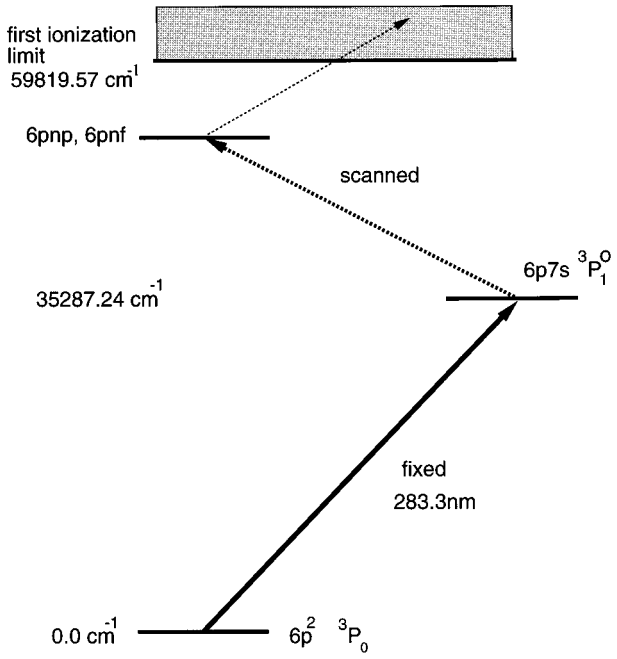

FIG. 2. Grotrian diagram of resonance ionization spectroscopy scheme in Pb.

lifetime of the state is 5.7 ns [22], and the isotope shifts (units of 10^{-3} cm^{-1}) relative to ^{208}Pb are the ^{204}Pb(-140.5), ^{206}Pb(-74.3), and ^{207}Pb(-46.4) center of gravity [24,25]. The hyperfine interaction constant (units of 10^{-3} cm^{-1}) of the state is ^{207}Pb($A=293.8$) [24,25].

II. EXPERIMENT

A. Experimental setup

An experimental setup consists of several parts: laser system and optical configuration, electro-thermal atomization, vacuum chamber, linear time-of-flight mass spectrometer, ion detection, and data acquisition instruments. Figure 1 shows the experimental setup used for this study.

For the first excitation step, a frequency-doubled (532-nm) neodymium-doped yttrium aluminum garnet (Nd:YAG) (Continuum, Surelite I) pumped dye laser (Continuum, ND60) was used to generate photons of 566.6-nm wavelength. The wavelength was frequency-doubled to 283.3 nm by a barium borate (BBO) crystal (Cleveland Crystals) in order to resonantly excite the $6p(^3P^o_{1/2})7s\ ^3P^o_1$ state. The 566.6-nm wavelength photons were separated by a harmonic separator (RMI). A XeCl excimer laser (Lambda Physik EMG201MSC) pumped dye laser (Lambda Physik FL3002) was used for the second excitation and/or ionization step. The second exciting laser frequency was calibrated with a Ne optogalvanic spectrum [26] and transmission fringes of a 0.67-cm^{-1} free-spectral-range étalon.

Atomic vapor of Pb was generated by a resistively heated tungsten heater. The vapor was collimated with a 1-mm pinhole to introduce it into the interaction region as an atomic beam. The temperature of the heater was controlled by an electric current of a dc power supply.

The laser beams intersected the atomic beam of Pb in the interaction region. The atoms excited by two-color resonance were ionized by another photon of the second laser or a negative pulsed electric field. The pulsed electric field after photon-atom interaction prevented atomic levels from a dc Stark shift. The ions were extracted by the same pulsed electric field from the interaction region in order to introduce them into a linear time-of-flight (TOF) mass spectrometer. The basic idea of the linear TOF was described in Ref. [27]. The ions were separated into each isotope through a 1.5-m drift tube of the TOF mass spectrometer. The vacuum chamber was pumped by two sets of a rotary pump and a turbo-

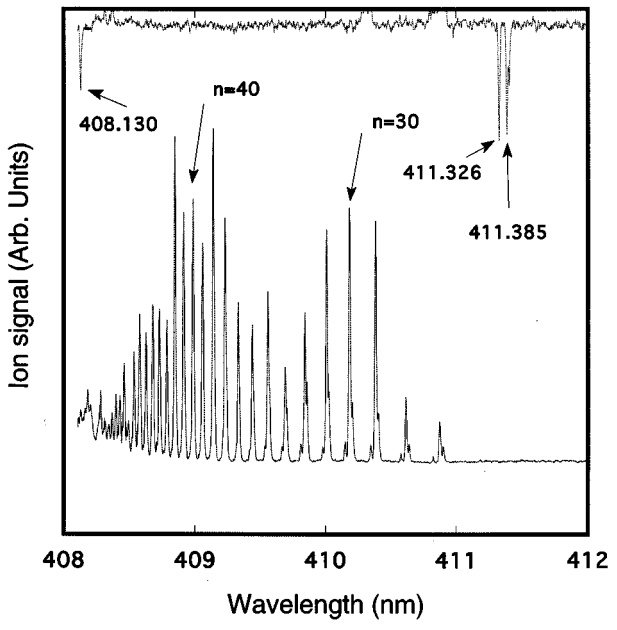

FIG. 3. Resonance ionization spectrum of Pb even-parity Rydberg series.

TABLE I. Experimental and theoretical term values, and assignment of $J=0$ even-parity $6pnp$ Rydberg series. The theoretical term values are calculated with the obtained MQDT parameters. (a) Three parameters; (b) five parameters, including energy-dependent terms. All values are given in cm^{-1}.

Configuration	E_{expt}	Standard deviation	E_{theor} (a)	E_{theor} (b)
$6p7p\ (\frac{1}{2},\frac{1}{2})$	44 401.13	0.20	44 865.324	44 401.709
$6p8p\ (\frac{1}{2},\frac{1}{2})$	51 781.02	0.11	51 840.752	51 779.164
$6p9p\ (\frac{1}{2},\frac{1}{2})$	54 861.81	0.21	54 869.691	54 863.274
$6p10p\ (\frac{1}{2},\frac{1}{2})$	56 450.77	0.25	56 451.905	56 455.161
$6p11p\ (\frac{1}{2},\frac{1}{2})$	57 381.06	0.13	57 381.021	57 385.520
$6p12p\ (\frac{1}{2},\frac{1}{2})$	57 968.05	0.24	57 972.639	57 976.674
$6p13p\ (\frac{1}{2},\frac{1}{2})$	58 383.94	0.28	58 372.429	58 375.737
$6p14p\ (\frac{1}{2},\frac{1}{2})$	58 654.15	0.17	58 655.174	58 657.834
$6p15p\ (\frac{1}{2},\frac{1}{2})$	58 861.90	0.12	58 862.475	58 864.617
$6p16p\ (\frac{1}{2},\frac{1}{2})$	59 016.34	0.77	59 018.967	59 020.712
$6p17p\ (\frac{1}{2},\frac{1}{2})$	59 139.66	0.61	59 139.993	59 141.427
$6p18p\ (\frac{1}{2},\frac{1}{2})$	59 234.45	0.27	59 235.512	59 236.704
$6p19p\ (\frac{1}{2},\frac{1}{2})$	59 312.69	0.37	59 312.220	59 313.218
$6p20p\ (\frac{1}{2},\frac{1}{2})$	59 374.69	0.13	59 374.750	59 375.595
$6p21p\ (\frac{1}{2},\frac{1}{2})$	59 425.65	0.25	59 426.393	59 427.118
$6p22p\ (\frac{1}{2},\frac{1}{2})$	59 469.33	0.13	59 469.536	59 470.166
$6p23p\ (\frac{1}{2},\frac{1}{2})$	59 505.75	0.18	59 505.947	59 506.498
$6p24p\ (\frac{1}{2},\frac{1}{2})$	59 536.26	0.16	59 536.957	59 537.445
$6p25p\ (\frac{1}{2},\frac{1}{2})$	59 563.61	0.26	59 563.583	59 564.024
$6p26p\ (\frac{1}{2},\frac{1}{2})$	59 586.01	0.10	59 586.615	59 587.015
$6p27p\ (\frac{1}{2},\frac{1}{2})$	59 606.31	0.18	59 606.671	59 607.031
$6p28p\ (\frac{1}{2},\frac{1}{2})$	59 623.79	0.29	59 624.242	59 624.575
$6p29p\ (\frac{1}{2},\frac{1}{2})$	59 639.61	0.18	59 639.722	59 640.030
$6p30p\ (\frac{1}{2},\frac{1}{2})$	59 653.26	0.09	59 653.430	59 653.726
$6p31p\ (\frac{1}{2},\frac{1}{2})$	59 665.42	0.11	59 665.625	59 665.904
$6p32p\ (\frac{1}{2},\frac{1}{2})$	59 676.36	0.07	59 676.521	59 676.788
$6p33p\ (\frac{1}{2},\frac{1}{2})$	59 686.08	0.13	59 686.296	59 686.563
$6p34p\ (\frac{1}{2},\frac{1}{2})$	59 694.84	0.03	59 695.095	59 695.358
$6p35p\ (\frac{1}{2},\frac{1}{2})$	59 702.89	0.14	59 703.042	59 703.318
$6p7p\ (\frac{3}{2},\frac{3}{2})$	59 705.51	0.26	59 705.379	59 705.381
$6p36p\ (\frac{1}{2},\frac{1}{2})$	59 710.06	0.12	59 710.237	59 710.526
$6p37p\ (\frac{1}{2},\frac{1}{2})$	59 716.56	0.19	59 716.762	59 717.096
$6p38p\ (\frac{1}{2},\frac{1}{2})$	59 722.67	0.13	59 722.669	59 723.080
$6p39p\ (\frac{1}{2},\frac{1}{2})$	59 728.03	0.26	59 727.942	59 728.562
$6p40p\ (\frac{1}{2},\frac{1}{2})$	59 733.12	0.07	59 732.242	59 733.582
$6p41p\ (\frac{1}{2},\frac{1}{2})$	59 737.65	0.17	59 738.729	59 738.203
$6p42p\ (\frac{1}{2},\frac{1}{2})$	59 741.72	0.21	59 742.702	59 742.455
$6p43p\ (\frac{1}{2},\frac{1}{2})$	59 745.86	0.35	59 746.529	59 746.391
$6p44p\ (\frac{1}{2},\frac{1}{2})$	59 749.41	0.19	59 750.116	59 750.030
$6p45p\ (\frac{1}{2},\frac{1}{2})$	59 753.26	0.12	59 753.460	59 753.403
$6p46p\ (\frac{1}{2},\frac{1}{2})$	59 756.28	0.48	59 756.576	59 756.532
$6p47p\ (\frac{1}{2},\frac{1}{2})$	59 759.15	0.43	59 759.480	59 759.456
$6p48p\ (\frac{1}{2},\frac{1}{2})$	59 761.43	0.58	59 762.190	59 762.177
$6p49p\ (\frac{1}{2},\frac{1}{2})$	59 764.32	0.48	59 764.722	59 764.714
$6p50p\ (\frac{1}{2},\frac{1}{2})$	59 766.65	0.13	59 767.091	59 767.088

molecular pump. The pressure of the vacuum chamber was typically 10^{-6}–10^{-7} Torr.

The ion signal detected by a microchannel plate (MCP) was fed into a gated integrator and boxcar averager (Stanford Research Systems SR250) via an amplifier (EG&G ORTEC 574), and the output signal from the boxcar averager was recorded as a function of the wavelength of the scanning laser in a computer through an analog-to-digital converter (Stanford Research Systems SR245). The output signals from the Ne optogalvano cell and a photodiode signal detecting the transmission fringes of the étalon were simultaneously recorded through the gated boxcar averager for the calibration of the wavelength of the scanning laser. The ex-

citation scheme of even-parity Rydberg series via the $6p(^3P^o_{1/2})7s\ ^3P^o_1$ is shown in Fig. 2. The intermediate state, 35 287.24 cm^{-1}, was excited by the frequency-doubled laser light described previously. The J values of the observed states were assigned by the method of polarization spectroscopy.

B. Measurements and determination of energy values

Figure 3 shows an example of the resonance ionization spectrum of Pb converging to the first ionization limit. The excited atoms were ionized by the pulsed electric field. The spectrum indicated in Fig. 3 is the output signal of the Ne optogalvano cell. This spectrum determines the absolute wavelength of the scanning laser. The wavelength between the two Ne absorption lines was calibrated by the transmission fringes of the étalon that were too fine to show in Fig. 3. The results of the energy values of even-parity Rydberg states of $J=0$, 1, and 2 are summarized in Tables, I, II, and III, respectively.

III. THEORETICAL ANALYSIS

Detailed descriptions of MQDT have been presented in many works, as described in the Introduction. We only summarize the procedure to obtain the MQD parameters.

In the Rydberg formula, the excited states of the ionic core can be considered by the definitions

$$E=I_i-\frac{R}{2\nu_i^2}=I_j-\frac{R}{2\nu_j^2}, \tag{1}$$

where I_i, ν_i are the ith ionization limit and corresponding effective quantum number, respectively, and R is the reduced-mass corrected Rydberg constant.

In MQDT, the two different bases play an important role to form the wave function of the Rydberg states. For the long-range interaction $r>r_0$, the theory uses the basis of ''collision channel'' that can be divided into the ionic core and the electron moving far from the core in the Coulomb field. On the other hand, the basis that expresses the short-range electron-ion (electron-electron) interactions in the region of $r<r_0$ is represented by a ''close-coupling channel.'' Two bases are connected at $r=r_0$.

For the discrete spectrum, the main condition of the boundary condition at $r=\infty$ leads to the condition

$$\sum_\alpha U_{i\alpha}\sin\pi(\nu_i+\mu_\alpha)A_\alpha=0. \tag{2}$$

For the nontrivial solutions for A_α, the condition

$$\det|U_{i\alpha}\sin\pi(\nu_i+\mu_\alpha)|=0 \tag{3}$$

is required.

In order to determine the quantum defect μ_α and the transformation matrix $U_{i\alpha}$ as parameters, Eq. (3), which describes a relationship between the effective quantum number ν_i and the parameters, must be fitted by using the experimental values.

In addition to providing a means of fitting experimentally determined eigenstate energies, MQDT provides detailed in

TABLE II. Experimental and theoretical term values, and assignment of $J=1$ even-parity Rydberg series. Observed terms are $6pnp\ (\frac{1}{2},\frac{3}{2})_1$, $6p7p\ (\frac{3}{2},\frac{1}{2})_1$, and $6p7p\ (\frac{3}{2},\frac{3}{2})_1$ Rydberg states. The theoretical term values are calculated with the obtained MQDT parameters. All values are given in cm^{-1}.

Configuration	E_{expt}	Standard deviation	E_{theor}
$6p7p\ (\frac{1}{2},\frac{1}{2})$	42 918.643[a]		42 916.54
$6p7p\ (\frac{1}{2},\frac{1}{2})$	44 674.9859[a]		44 580.94
$6p8p\ (\frac{1}{2},\frac{1}{2})$	51 320.598[a]		51 320.45
$6p8p\ (\frac{1}{2},\frac{1}{2})$	51 911.19	0.11	51 914.11
$6p9p\ (\frac{1}{2},\frac{1}{2})$	54 653.72[a]		54 654.19
$6p9p\ (\frac{1}{2},\frac{3}{2})$	54 928.0835[a]		54 927.31
$6p10p\ (\frac{1}{2},\frac{1}{2})$	56 338.932[a]		56 333.35
$6p10p\ (\frac{1}{2},\frac{3}{2})$	56 475.35	0.19	56 478.86
$6p7p\ (\frac{3}{2},\frac{1}{2})$	57 010.16	0.15	57 010.19
$6p11p\ (\frac{1}{2},\frac{1}{2})$	57 317.841[a]		57 327.48
$6p11p\ (\frac{1}{2},\frac{3}{2})$	57 430.27	0.07	57 425.61
$6p12p\ (\frac{1}{2},\frac{1}{2})$	57 916.086[a]		57 928.09
$6p12p\ (\frac{1}{2},\frac{3}{2})$	57 993.98	0.31	57 994.24
$6p7p\ (\frac{3}{2},\frac{3}{2})$	58 324.46	0.20	58 310.90
$6p13p\ (\frac{1}{2},\frac{1}{2})$			58 379.67
$6p13p\ (\frac{1}{2},\frac{3}{2})$	58 402.61	0.23	58 462.76
$6p14p\ (\frac{1}{2},\frac{1}{2})$			58 648.61
$6p14p\ (\frac{1}{2},\frac{3}{2})$	58 669.71	0.21	58 675.65
$6p15p\ (\frac{1}{2},\frac{1}{2})$			58 854.93
$6p15p\ (\frac{1}{2},\frac{3}{2})$	58 872.56	0.17	58 875.09
$6p16p\ (\frac{1}{2},\frac{1}{2})$			59 012.41
$6p16p\ (\frac{1}{2},\frac{3}{2})$	59 024.27	0.64	59 028.09
$6p17p\ (\frac{1}{2},\frac{1}{2})$			59 134.30
$6p17p\ (\frac{1}{2},\frac{3}{2})$	59 147.33	0.33	59 146.95
$6p18p\ (\frac{1}{2},\frac{1}{2})$			59 225.78
$6p18p\ (\frac{1}{2},\frac{3}{2})$	59 239.07	0.21	59 239.47
$6p5f\ \frac{3}{2}[\frac{3}{2}]$			59 242.31
$6p19p\ (\frac{1}{2},\frac{1}{2})$			59 309.45
$6p19p\ (\frac{1}{2},\frac{3}{2})$	59 315.58	0.24	59 316.71
$6p20p\ (\frac{1}{2},\frac{1}{2})$			59 372.26
$6p20p\ (\frac{1}{2},\frac{3}{2})$	59 377.98	0.16	59 378.42
$6p21p\ (\frac{1}{2},\frac{1}{2})$			59 424.26
$6p21p\ (\frac{1}{2},\frac{3}{2})$	59 429.33	0.25	59 429.44
$6p22p\ (\frac{1}{2},\frac{1}{2})$			59 467.73
$6p22p\ (\frac{1}{2},\frac{3}{2})$	59 471.53	0.15	59 472.11
$6p23p\ (\frac{1}{2},\frac{1}{2})$			59 504.41
$6p23p\ (\frac{1}{2},\frac{3}{2})$	59 508.23	0.15	59 508.13
$6p24p\ (\frac{1}{2},\frac{1}{2})$			59 535.65
$6p24p\ (\frac{1}{2},\frac{3}{2})$	59 538.51	0.17	59 538.84
$6p25p\ (\frac{1}{2},\frac{1}{2})$			59 562.46
$6p25p\ (\frac{1}{2},\frac{3}{2})$	59 565.22	0.30	59 565.22
$6p26p\ (\frac{1}{2},\frac{1}{2})$			59 585.65
$6p26p\ (\frac{1}{2},\frac{3}{2})$			59 588.04
$6p27p\ (\frac{1}{2},\frac{1}{2})$			59 605.84
$6p27p\ (\frac{1}{2},\frac{3}{2})$	59 607.94	0.19	59 607.93
$6p28p\ (\frac{1}{2},\frac{1}{2})$			59 623.52
$6p28p\ (\frac{1}{2},\frac{3}{2})$			59 625.36
$6p29p\ (\frac{1}{2},\frac{1}{2})$			59 639.10
$6p29p\ (\frac{1}{2},\frac{3}{2})$			59 640.73
$6p30p\ (\frac{1}{2},\frac{1}{2})$			59 652.89
$6p30p\ (\frac{1}{2},\frac{3}{2})$			59 654.34

[a]Values from Wood and Andrew [17].

TABLE III. Experimental and theoretical term values, and assignment of $J=2$ even-parity $6pnp$ and $6pnf$ Rydberg series. The theoretical term values are calculated with the obtained MQDT parameters. All values are given in cm^{-1}.

Configuration	E_{expt}	Standard deviation	E_{theor}	Configuration	E_{expt}	Standard deviation	E_{theor}
$6p7p\ (\frac{1}{2},\frac{3}{2})$	44 810.01	0.21	44 808.26	$6p30f\ ^1_2[\frac{5}{2}]$	59 688.57	0.21	59 688.55
$6p8p\ (\frac{1}{2},\frac{3}{2})$	51 938.63	0.11	51 938.54	$6p34p\ (\frac{1}{2},\frac{3}{2})$	59 695.90	0.12	59 696.13
$6p5f\ ^1_2[\frac{5}{2}]$	52 841.82[a]		52 850.79	$6p31f\ ^1_2[\frac{5}{2}]$	59 697.45	0.25	59 697.12
$6p9p\ (\frac{1}{2},\frac{3}{2})$	54 929.57	0.26	54 929.50	$6p35p\ (\frac{1}{2},\frac{3}{2})$	59 703.85	0.10	59 704.01
$6p6f\ ^1_2[\frac{5}{2}]$	55 360.077[a]		55 360.10	$6p32f\ ^1_2[\frac{5}{2}]$	59 705.51	0.26	59 704.87
$6p10p\ (\frac{1}{2},\frac{3}{2})$	56 467.63	0.12	56 467.69	$6p36p\ (\frac{1}{2},\frac{3}{2})$	59 711.11	0.14	59 711.16
$6p7f\ ^1_2[\frac{5}{2}]$	56 719.794[a]		56 719.78	$6p33f\ ^1_2[\frac{5}{2}]$	59 712.01	0.06	59 711.90
$6p11p\ (\frac{1}{2},\frac{3}{2})$	57 260.668[a]		57 260.55	$6p37p\ (\frac{1}{2},\frac{3}{2})$	59 717.51	0.07	59 717.66
$6p8f\ ^1_2[\frac{5}{2}]$	57 497.795[a]		57 499.78	$6p34f\ ^1_2[\frac{5}{2}]$	59 718.56	0.11	59 718.30
$6p7p\ (\frac{3}{2},\frac{1}{2})$	57 598.65	0.17	57 599.63	$6p38p\ (\frac{1}{2},\frac{3}{2})$	59 723.51	0.16	59 723.59
$6p12p\ (\frac{1}{2},\frac{3}{2})$	58 008.62	0.21	58 013.13	$6p35f\ ^1_2[\frac{5}{2}]$	59 724.43	0.09	59 724.14
$6p9f\ ^1_2[\frac{5}{2}]$			58 093.27	$6p39p\ (\frac{1}{2},\frac{3}{2})$	59 728.82	0.09	59 729.03
$6p13p\ (\frac{1}{2},\frac{3}{2})$	58 397.77	0.30	58 392.46	$6p36f\ ^1_2[\frac{5}{2}]$	59 729.89	0.32	59 729.48
$6p10f\ ^1_2[\frac{5}{2}]$			58 453.75	$6p40p\ (\frac{1}{2},\frac{3}{2})$	59 733.99	0.11	59 734.01
$6p14p\ (\frac{1}{2},\frac{3}{2})$	58 666.67	0.18	58 662.57	$6p37f\ ^1_2[\frac{5}{2}]$	59 734.83	0.44	59 734.37
$6p11f\ ^1_2[\frac{5}{2}]$			58 712.55	$6p41p\ (\frac{1}{2},\frac{3}{2})$	59 738.57	0.29	59 738.59
$6p15p\ (\frac{1}{2},\frac{3}{2})$			58 853.96	$6p38f\ ^1_2[\frac{5}{2}]$	59 738.82	0.42	59 738.87
$6p12f\ ^1_2[\frac{5}{2}]$			58 903.51	$6p42p\ (\frac{1}{2},\frac{3}{2})$	59 742.30	0.40	59 742.81
$6p7p\ (\frac{3}{2},\frac{3}{2})$	58 971.32	0.26	58 973.50	$6p39f\ ^1_2[\frac{5}{2}]$	59 742.96	0.26	59 743.01
$6p16p\ (\frac{1}{2},\frac{3}{2})$	59 041.46	0.29	59 046.82	$6p43p\ (\frac{1}{2},\frac{3}{2})$	59 746.24	0.29	59 746.69
$6p13f\ ^1_2[\frac{5}{2}]$			59 066.21	$6p40f\ ^1_2[\frac{5}{2}]$	59 746.74	0.25	59 746.82
$6p17p\ (\frac{1}{2},\frac{3}{2})$	59 152.77	0.21	59 157.60	$6p44p\ (\frac{1}{2},\frac{3}{2})$	59 750.01	0.23	59 750.25
$6p14f\ ^1_2[\frac{5}{2}]$			59 169.07	$6p41f\ ^1_2[\frac{5}{2}]$	59 750.69	0.42	59 750.38
$6p18p\ (\frac{1}{2},\frac{3}{2})$	59 244.12	0.24	59 247.57	$6p45p\ (\frac{1}{2},\frac{3}{2})$	59 753.63	0.26	59 753.48
$6p15f\ ^1_2[\frac{5}{2}]$			59 256.61	$6p42f\ ^1_2[\frac{5}{2}]$	59 753.80	0.31	59 753.71
$6p5f\ ^3_2[\frac{3}{2}]$[b]			59 313.84	$6p46p\ (\frac{1}{2},\frac{3}{2})$	59 756.36	0.17	59 756.45
$6p19p\ (\frac{1}{2},\frac{3}{2})$	59 318.47	0.36	59 322.20	$6p43f\ ^1_2[\frac{5}{2}]$	59 756.83	0.30	59 756.82
$6p16f\ ^1_2[\frac{5}{2}]$			59 335.15	$6p47p\ (\frac{1}{2},\frac{3}{2})$	59 759.53	0.35	59 759.16
$6p20p\ (\frac{1}{2},\frac{3}{2})$	59 380.16	0.18	59 382.03	$6p44f\ ^1_2[\frac{5}{2}]$	59 759.83	0.27	59 759.71
$6p17f\ ^1_2[\frac{5}{2}]$			59 390.25	$6p48p\ (\frac{1}{2},\frac{3}{2})$	59 761.99	0.52	59 761.67
$6p21p\ (\frac{1}{2},\frac{3}{2})$	59 431.29	0.17	59 432.21	$6p45f\ ^1_2[\frac{5}{2}]$	59 762.26	0.52	59 762.41
$6p18f\ ^1_2[\frac{5}{2}]$			59 438.87	$6p49p\ (\frac{1}{2},\frac{3}{2})$	59 764.55	0.49	59 764.01
$6p22p\ (\frac{1}{2},\frac{3}{2})$	59 473.20	0.08	59 474.31	$6p46f\ ^1_2[\frac{5}{2}]$	59 764.79	0.50	59 764.93
$6p19f\ ^1_2[\frac{5}{2}]$			59 479.86	$6p50p\ (\frac{1}{2},\frac{3}{2})$	59 767.05	0.02	59 766.23
$6p23p\ (\frac{1}{2},\frac{3}{2})$	59 509.20	0.16	59 509.93	$6p47f\ ^1_2[\frac{5}{2}]$	59 767.43	0.22	59 767.29
$6p20f\ ^1_2[\frac{5}{2}]$			59 514.62	$6p51p\ (\frac{1}{2},\frac{3}{2})$			59 768.36
$6p24p\ (\frac{1}{2},\frac{3}{2})$	59 539.34	0.15	59 540.32	$6p48f\ ^1_2[\frac{5}{2}]$	59 769.72	0.33	59 769.50
$6p21f\ ^1_2[\frac{5}{2}]$			59 544.32	$6p52p\ (\frac{1}{2},\frac{3}{2})$	59 770.35	0.23	59 770.39
$6p25p\ (\frac{1}{2},\frac{3}{2})$	59 556.06	0.13	59 566.46	$6p49f\ ^1_2[\frac{5}{2}]$	59 771.71	0.22	59 771.57
$6p22f\ ^1_2[\frac{5}{2}]$			59 569.89	$6p53p\ (\frac{1}{2},\frac{3}{2})$	59 772.41	0.24	59 772.33
$6p26p\ (\frac{1}{2},\frac{3}{2})$	59 588.08	0.21	59 589.10	$6p50f\ ^1_2[\frac{5}{2}]$	59 773.37	0.22	59 773.52
$6p23f\ ^1_2[\frac{5}{2}]$	59 591.93	0.14	59 592.05	$6p54p\ (\frac{1}{2},\frac{3}{2})$	59 773.67	0.29	59 774.18
$6p27p\ (\frac{1}{2},\frac{3}{2})$	59 608.44	0.20	59 608.84	$6p51f\ ^1_2[\frac{5}{2}]$	59 775.22	0.17	59 775.35
$6p24f\ ^1_2[\frac{5}{2}]$	59 611.39	0.17	59 611.39	$6p55p\ (\frac{1}{2},\frac{3}{2})$	59 775.51	0.20	59 775.93
$6p28p\ (\frac{1}{2},\frac{3}{2})$	59 625.79	0.14	59 626.15	$6p52f\ ^1_2[\frac{5}{2}]$			59 777.07
$6p25f\ ^1_2[\frac{5}{2}]$	59 628.65	0.14	59 628.37	$6p56p\ (\frac{1}{2},\frac{3}{2})$			59 777.59
$6p29p\ (\frac{1}{2},\frac{3}{2})$	59 641.16	0.15	59 641.41	$6p53f\ ^1_2[\frac{5}{2}]$			59 778.69
$6p26f\ ^1_2[\frac{5}{2}]$	59 643.60	0.17	59 643.34	$6p57p\ (\frac{1}{2},\frac{3}{2})$			59 779.17
$6p30p\ (\frac{1}{2},\frac{3}{2})$	59 654.67	0.17	59 654.94	$6p54f\ ^1_2[\frac{5}{2}]$			59 780.23
$6p27f\ ^1_2[\frac{5}{2}]$	59 656.85	0.19	59 656.62	$6p58p\ (\frac{1}{2},\frac{3}{2})$			59 780.66
$6p31p\ (\frac{1}{2},\frac{3}{2})$	59 666.74	0.17	59 666.98	$6p55f\ ^1_2[\frac{5}{2}]$			59 781.67
$6p28f\ ^1_2[\frac{5}{2}]$	59 668.59	0.16	59 668.46	$6p59p\ (\frac{1}{2},\frac{3}{2})$			59 782.07
$6p32p\ (\frac{1}{2},\frac{3}{2})$	59 677.47	0.16	59 677.75	$6p56f\ ^1_2[\frac{5}{2}]$			59 783.04
$6p29f\ ^1_2[\frac{5}{2}]$	59 679.22	0.14	59 679.04	$6p60p\ (\frac{1}{2},\frac{3}{2})$			59 783.41
$6p33p\ (\frac{1}{2},\frac{3}{2})$	59 687.26	0.14	59 687.42				

[a]Values from Wood and Andrew [17].

[b]This assignment is determined from the admixture coefficient

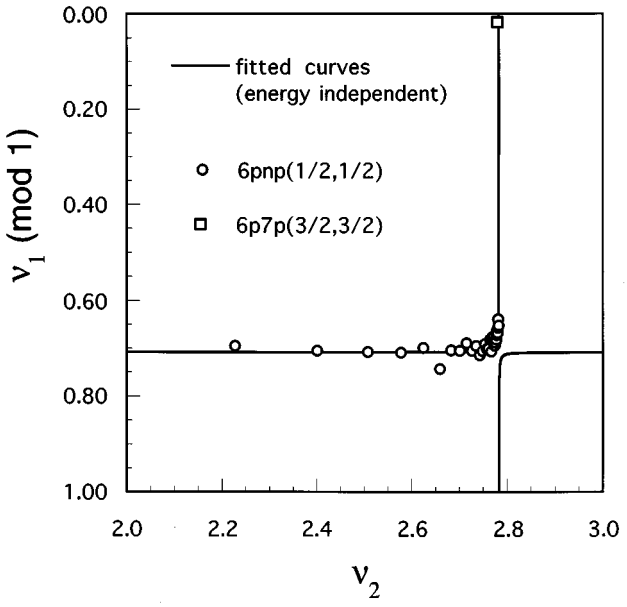

FIG. 4. Lu-Fano plot for $J=0$ even-parity levels.

formation on the extent of configuration mixing that occurs in these eigenstates. Although the Ψ_α eigenchannels are, in general, mixed configurations, the i collision channels are all pure configurations. The admixture of configurations is thus given by

$$Z_i^{(n)}=(-1)^{(I_i+1)}\nu_i^{3/2}\sum_\alpha U_{i\alpha}\cos\pi(\nu_i^{(n)}+\mu_\alpha)A^{(n)}/N_n\,, \tag{4}$$

where $Z_i^{(n)}$ is the coefficient of the ith collision channel in the nth eigenstate $\Psi^{(n)}$ and N_n is a normalization factor.

IV. THEORETICAL ANALYSES

A. Analysis of the $J=0$, even-parity spectrum

The levels of $J=0$ even-parity Rydberg series identified by polarization spectroscopy are $6pnp(\frac{1}{2},\frac{1}{2})_0$ and $6pnp(\frac{3}{2},\frac{3}{2})_0$, of which $6pnp(\frac{1}{2},\frac{1}{2})_0$ ($28\leqslant n\leqslant 50$) and $6p7p(\frac{3}{2},\frac{3}{2})_0$ are newly observed and their energy values determined. The $J=0$, even-parity spectrum consists of two channels, one of which converges to the first ionization limit $^2P_{1/2}$ (59 819.57 cm^{-1}) and the other converges to the second ionization limit $^2P_{3/2}$ (73 900.64 cm^{-1}). Two channels can be labeled as

	Close coupling channels	
$\alpha=$	1	2
	$6pnp\ ^3P_0$	$6pnp\ ^1S_0$
	Collision channels	
$i=$	1	2
	$6pnp(\frac{1}{2},\frac{1}{2})_0$	$6pnp(\frac{3}{2},\frac{3}{2})_0$

The effective quantum numbers ν_1 and ν_2 calculated from the definition (1) are plotted in Fig. 4. In the case of two-channel problem, the transformation matrix $U_{i\alpha}$ can be written as

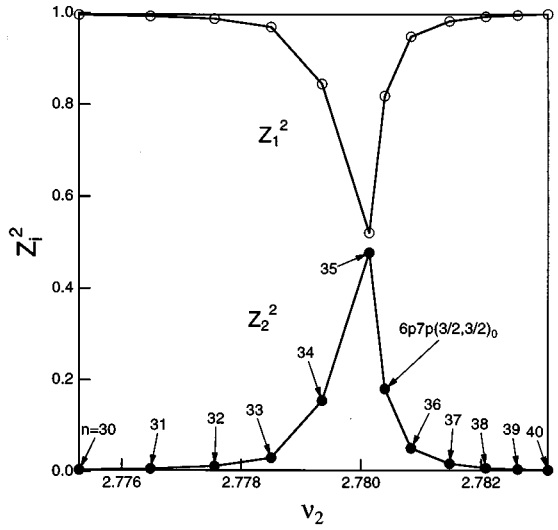

FIG. 5. Admixture coefficients Z_1 and Z_2 as a function of the effective quantum number ν_2.

$$U_{i\alpha}=\begin{pmatrix}\cos\theta & \sin\theta\\ -\sin\theta & \cos\theta\end{pmatrix}. \tag{5}$$

The number of the term values obtained by the experiment is enough to derive the multichannel quantum defect parameters μ_1, μ_2, θ by fitting the theoretical values to the experimental values. We also determine the parameters when including the energy-dependent parameters. The dependence of the parameters on the energy values will be discussed later. Using the parameters, we calculated the term values which are written in Table I.

Theoretical values of (μ_1,μ_2) are plotted in Fig. 4 as a line. Figure 4 shows that there is one state perturbing the $6pnp(\frac{1}{2},\frac{1}{2})_0$ series because the line in the figure is bent at $\nu_1\simeq 0.7$. This means that there is a $6pnp(\frac{3}{2},\frac{3}{2})_0$ perturbing level here. The perturbing level is identified as $6p7p(\frac{3}{2},\frac{3}{2})_0$ positioning on 59 705.51 cm^{-1}. The $6p7p(\frac{3}{2},\frac{3}{2})_0$ level is observed between $6p35p(\frac{1}{2},\frac{1}{2})_0$ and $6p36p(\frac{3}{2},\frac{3}{2})_0$, as predicted by Ding *et al.* [18]. The mixing between two Rydberg series is evaluated by the admixture coefficient defined by Eq. (4). The coefficients of Z_1 and Z_2 are plotted in Fig. 5. The figure shows that the mixing configuration is large around $6p35p(\frac{1}{2},\frac{1}{2})_0$ due to the perturbation of the $6p7p(\frac{3}{2},\frac{3}{2})_0$ level.

B. Analysis of the $J=1$, even-parity spectrum

We assigned the $J=1$ $6pnp(\frac{1}{2},\frac{3}{2})_1$, $6p7p(\frac{3}{2},\frac{1}{2})_1$, and $6p7p(\frac{3}{2},\frac{3}{2})_1$. Also identified of these levels are $6pnp(\frac{1}{2},\frac{3}{2})_1$ ($14\leqslant n\leqslant 27$) Rydberg series by the two-color resonance ionization spectroscopy.

The collision channels of the $J=1$, even parity levels are labeled as

$i=$	1	2	3	4	5
	$6pnp$ $(\frac{1}{2},\frac{1}{2})_1$,	$6pnp$ $(\frac{1}{2},\frac{3}{2})_1$,	$6pnp$ $(\frac{3}{2},\frac{3}{2})_1$,	$6pnp$ $(\frac{3}{2},\frac{1}{2})_1$,	$6pnf$ $^3_2[\frac{3}{2}]_1$

The first two channels converge to the first ionization limit $^2P_{1/2}$, while the other three channels converge to the second ionization limit $^2P_{3/2}$.

We should simplify Eq. (3) first for the purpose of analyzing the spectrum. The five equations (3) are reduced to two equations by the substitution [5]

$$A_\alpha=\frac{1}{\sin\pi(\nu_2+\mu_\alpha)}\sum_{j=1}^{2}U^\dagger_{\alpha j}B_j, \tag{6}$$

which satisfies the equations of $i=3$, 4, and 5. These channels are the series converging to the second ionization limit I_2. The two equations (6) are written as

$$\sum_{j=1}^{2}\left[\sum_{\alpha=1}^{5}U_{i\alpha}\frac{\sin\pi(\nu_1+\mu_\alpha)}{\sin\pi(\nu_2+\mu_\alpha)}U^\dagger_{\alpha j}\right]B_j=0. \tag{7}$$

Using the transformation of the term in Eq. (7),

$$\begin{aligned}\frac{\sin\pi(\nu_1+\mu_\alpha)}{\sin\pi(\nu_2+\mu_\alpha)}&=\frac{\sin\pi[(\nu_1-\nu_2)+\nu_2+\mu_\alpha]}{\sin\pi(\nu_2+\mu_\alpha)}\\&=\sin\pi(\nu_1-\nu_2)\\&\quad\times\{\cot\pi(\nu_1-\nu_2)+\cot\pi(\nu_2+\mu_\alpha)\},\end{aligned} \tag{8}$$

we obtain the following equation from (7):

$$\sum_{j=1}^{2}[\cot\pi(\nu_1-\nu_2)\delta_{ij}+M_{ij}(\nu_2)]B_j=0, \tag{9}$$

where $M_{ij}(\nu_2)$ is

$$M_{ij}(\nu_2)=\sum_{\alpha=1}^{5}U_{i\alpha}\cot\pi(\nu_2+\mu_\alpha)U^\dagger_{\alpha j}. \tag{10}$$

The nontrivial solutions for B_j could be obtained if

$$\det|\cot\pi(\nu_1-\nu_2)\delta_{ij}+M_{ij}(\nu_2)|=0. \tag{11}$$

This can be expanded as

$$\begin{aligned}\cot^2\pi(\nu_1-\nu_2)+(M_{11}+M_{22})\cot\pi(\nu_1-\nu_2)+M_{11}M_{22}\\-M_{12}M_{21}=0,\end{aligned} \tag{12}$$

in the case of the $J=1$, even-parity spectrum of Pb. Solving Eq. (12), we derive ν_1 as a function of ν_2 as

$$\nu_1=\nu_2+\frac{1}{\pi}\cot^{-1}\chi_\pm, \tag{13}$$

where

$$\chi_\pm=\tfrac{1}{2}\{-(M_{11}+M_{22})\pm\sqrt{(M_{11}-M_{22})^2+4M_{12}M_{21}}\}. \tag{14}$$

The transformation matrix $U_{i\alpha}$ between the close-coupling channels and the collision channels is a unitary matrix. The matrix is generated by the rotations of the combinations from a geometrical point of view [6]. In the case of five channels, the number of the combinations is 10. Generally the $n\times n$ transformation matrix, therefore, can be expressed as

$$U_{i\alpha}=\prod_{\beta=1}^{n(n-1)/2}V_\beta(\theta_\beta), \tag{15}$$

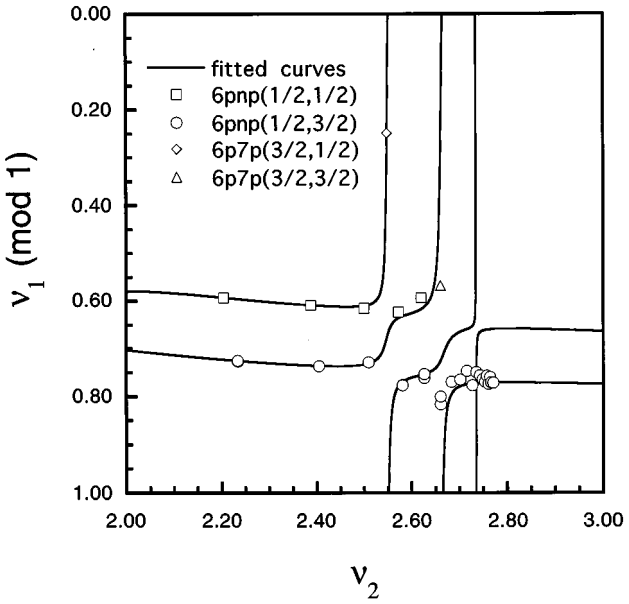

FIG. 6. Lu-Fano plot for $J=1$ even-parity levels.

where the combination of $\beta=(i,j)$ is written as

$$V_\beta(\phi_\beta)=\begin{array}{c|cccccccc} & 1 & 2 & \cdot & i & \cdot & j & \cdot & n\\ 1 & 1 & 0 & 0 & 0 & 0 & 0 & 0 & 0\\ 2 & 0 & 1 & 0 & 0 & 0 & 0 & 0 & 0\\ \cdot & \cdot & \cdot & \cdot & \cdot & \cdot & \cdot & \cdot & \cdot\\ i & 0 & 0 & 0 & \cos\phi_\beta & 0 & -\sin\phi_\beta & 0 & 0\\ \cdot & \cdot & \cdot & \cdot & \cdot & \cdot & \cdot & \cdot & \cdot\\ j & 0 & 0 & 0 & \sin\phi_\beta & 0 & \cos\phi_\beta & 0 & 0\\ \cdot & \cdot & \cdot & \cdot & \cdot & \cdot & \cdot & \cdot & \cdot\\ n & 0 & 0 & 0 & 0 & 0 & 0 & 0 & 1\end{array} \tag{16}$$

The energy dependence of the parameters was discussed to treat a broader energy range [4,6]. The parameters μ_α and θ_β can be expanded linearly into the power of the energy ϵ measured from the lowest ionization limit,

$$\mu_\alpha=\mu^0_\alpha+\epsilon\mu^1_\alpha, \tag{17}$$

$$\theta_\beta=\theta^0_\beta+\epsilon\theta^1_\beta. \tag{18}$$

The energy dependence of the quantum defects μ^1_α is taken into account here.

The two effective quantum numbers ν_1 and ν_2 for $J=1$ converging to the first and second ionization limits, respectively, are plotted in Fig. 6. The multichannel quantum defect parameters were determined by a nonlinear fitting method for the theoretical curves to trace the experimental term values as closely as possible in Fig. 6.

The theoretical term values calculated by the parameters are written next to the experimental values in Table II. The theoretical term values are given by the simultaneous solutions of Eqs. (1) and (13).

The root mean square (rms) between the experimental and theoretical term values is 4.08 cm^{-1}. The value could be

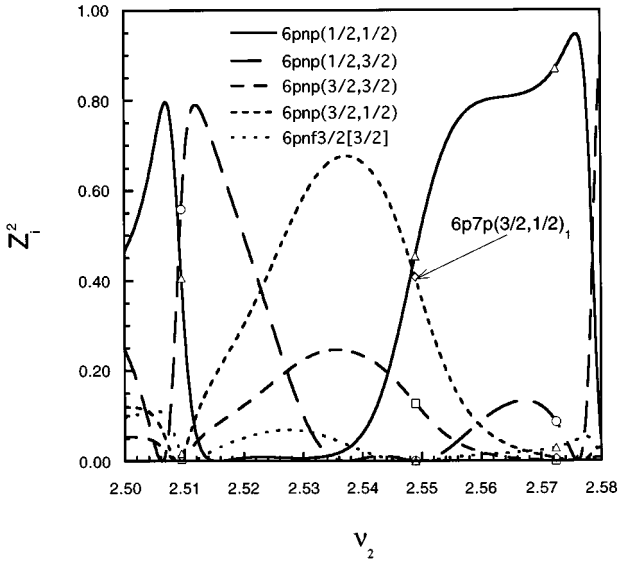

FIG. 7. Admixture coefficients at 57 010 cm^{-1} $[6p7p(\frac{3}{2},\frac{1}{2})_1]$ using the obtained parameters for $J=1$.

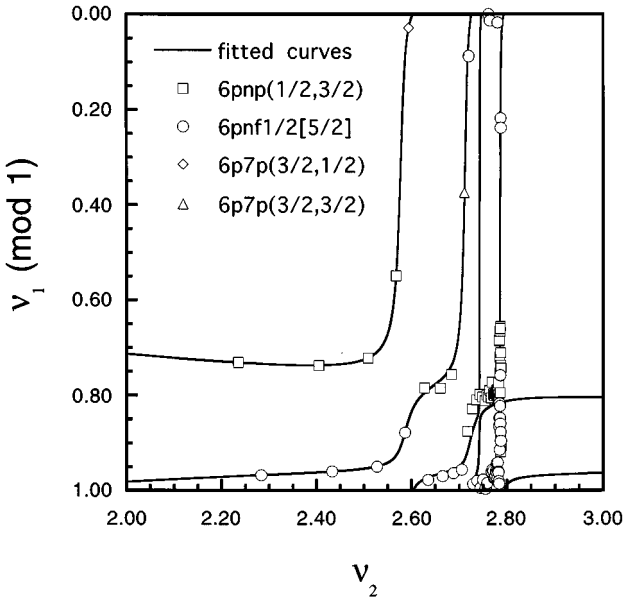

FIG. 8. Lu-Fano plot for $J=2$ even-parity levels.

improved by increasing the number of observed levels. The experimental term values are assigned by the theoretical term values using the admixture coefficients defined by Eq. (4).

We plot the admixture coefficients at 57 010 cm^{-1} in Fig. 7. This figure shows that the maximum admixture with $6pnp(\frac{3}{2},\frac{1}{2})_1$ occurs for the level at 57 010 cm^{-1} and the configuration is restricted to the level. The level also has a few characteristics of $6pnp(\frac{3}{2},\frac{1}{2})_1$. These result in the level at 57 010 cm^{-1} being labeled as $6p7p(\frac{3}{2},\frac{1}{2})_1$. In order to investigate the spectrum near the first ionization limit and access $6pnp(\frac{1}{2},\frac{1}{2})_1$ Rydberg series, higher resolution laser spectroscopy and other excitation methods for the first step such as electron excitation are required.

C. Analysis of the $J=2$, even-parity spectrum

We identified $J=2$ $6pnp(\frac{1}{2},\frac{3}{2})_2$, $6p7p(\frac{3}{2},\frac{1}{2})_2$, $6p7p(\frac{3}{2},\frac{3}{2})_2$, and $6pnf\ ^1_2[^5_2]_2$ even-parity Rydberg series. Other identified levels of the observed are $6pnp(\frac{1}{2},\frac{3}{2})_2$ $(42\leqslant n\leqslant 54)$ and $6pnf\ ^1_2[^5_2]_2$ $(28\leqslant n\leqslant 51)$.

The collision channels of the $J=2$, even-parity spectrum are labeled as

$i=$	1	2	3	4	5	6
	$6pnp$ $(\frac{1}{2},\frac{3}{2})_2$	$6pnf$ $^1_2[^5_2]_2$	$6pnp$ $(\frac{3}{2},\frac{3}{2})_2$	$6pnf$ $^3_2[^3_2]_2$	$6pnf$ $^3_2[^5_2]_2$	$6pnp$ $(\frac{3}{2},\frac{1}{2})_2$

The angular momentum of the valence f electron is so large that the $6pnf$ Rydberg series are classified in the jK coupling scheme. The effective quantum numbers defined by Eq. (1) are plotted in Fig. 8.

The multichannel quantum defect parameters are determined as the case of $J=1$ using a nonlinear fitting procedure. The lines in Fig. 8 are drawn with the fitted parameters. The theoretical term values in Table III are given by the simultaneous solutions of Eqs. (1) and (13) using these parameters. The rms between the theoretical and the experimental energy values is 0.19 cm^{-1}. The theoretical analyses helped to assign the experimental energy values.

We show the admixture coefficients at 57 598 cm^{-1} and 58 971 cm^{-1} in Figs. 9 and 10. These levels perturb the Rydberg series converging to the first ionization limit, which are shown in the Lu-Fano plot of Fig. 8.

Figure 9 shows that the level at 57 598 cm^{-1} has the maximum admixture with $6pnp(\frac{3}{2},\frac{1}{2})_2$, and the admixture coefficient of $6pnp(\frac{3}{2},\frac{1}{2})_2$ is confined to the level. It can, therefore, be labeled as $6p7p(\frac{3}{2},\frac{1}{2})_2$. On the other hand, the level at 58 971 cm^{-1} has the maximum value of admixture coefficient of $6pnp(\frac{3}{2},\frac{3}{2})_2$ and is labeled as $6p7p(\frac{3}{2},\frac{3}{2})_2$.

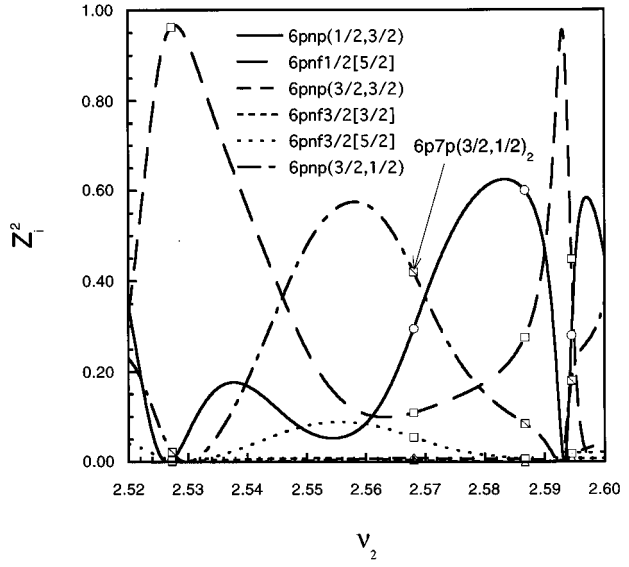

FIG. 9. Admixture coefficients at 57 598 cm^{-1} $[6p7p(\frac{3}{2},\frac{1}{2})_2]$ using the obtained parameters for $J=2$.

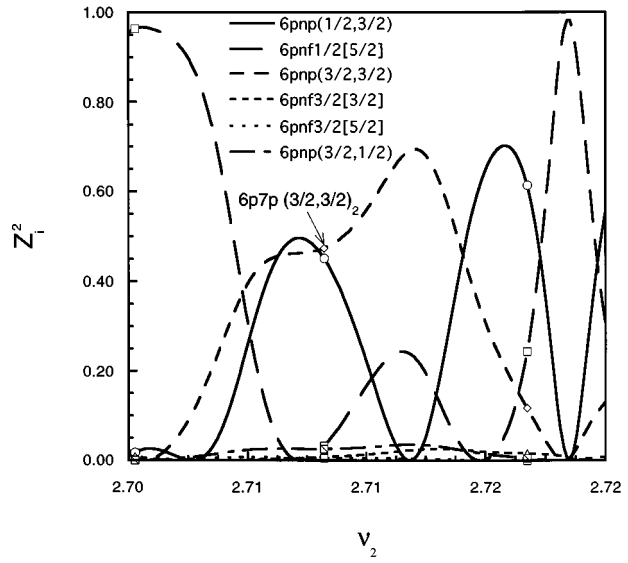

FIG. 10. Admixture coefficients at 58 971 cm^{-1} $[6p7p(\frac{3}{2},\frac{3}{2})_2]$ using the obtained parameters for $J=2$.

V. CONCLUSION

Exciting the $6p7s\ ^3P_1^0$ as the intermediate state, even-parity Rydberg series of atomic lead have been investigated. Applying multichannel quantum defect theory to the experimental data, the high-lying states below the first ionization limit have been assigned and the configuration interaction has been estimated.

The levels of the $J=0$, even-parity Rydberg series identified by the experiment are extended to $6pnp(\frac{1}{2},\frac{1}{2})_0$ ($28 \leqslant n \leqslant 50$) and $6p7p(\frac{3}{2},\frac{3}{2})_0$. The $6p7p(\frac{3}{2},\frac{3}{2})_0$ interloper state is identified at 59 705.51 cm^{-1} between $6p35p(\frac{1}{2},\frac{1}{2})_0$ and $6p36p(\frac{1}{2},\frac{1}{2})_0$. The multichannel quantum defect parameters for $J=0$, even-parity spectra were determined with the experimental values. Using the parameters, we calculated the admixture coefficients of $6pnp(\frac{1}{2},\frac{1}{2})_0$ and $6pnp(\frac{3}{2},\frac{3}{2})_0$. The results showed that the $6p35p(\frac{1}{2},\frac{1}{2})_0$ level has largest admixture coefficient, with the $6pnp(\frac{3}{2},\frac{3}{2})_0$ Rydberg series due to the $6p7p(\frac{3}{2},\frac{3}{2})_0$ perturber.

The Rydberg series of $J=1$ $6pnp(\frac{1}{2},\frac{3}{2})_1$ ($14 \leqslant n \leqslant 27$) are also identified by the two-color resonance ionization spectroscopy. Multichannel quantum defect parameters for the $J=1$, even-parity spectrum are obtained by a nonlinear fitting procedure. We have assigned the electronic configuration of the term values observed by the experiment using MQDT and calculated admixture coefficients to evaluate perturbation of $6p7p(\frac{3}{2},\frac{1}{2})_1$. Unobserved term values and assignments are predicted using MQDT parameters. Higher-resolution spectroscopy is required to investigate the levels near the ionization limit.

The observed levels of $J=2$ even parity Rydberg series by the experiment are $6pnp(\frac{1}{2},\frac{3}{2})_2$ ($42 \leqslant n \leqslant 54$) and $6pnf\ ^1[\frac{5}{2}]_2$ ($28 \leqslant n \leqslant 51$). With nonlinear fitting, multichannel quantum defect parameters are obtained for the $J=2$ even-parity spectrum. The experimental term values were compared with the theoretical values calculated by MQDT using the parameters. The correspondence between two values were so good that the observed peak could be assigned. The perturbing levels $6p7p(\frac{3}{2},\frac{1}{2})_2$ and $6p7p(\frac{3}{2},\frac{3}{2})_2$ are assigned with admixture coefficients using MQDT parameters. Further spectroscopic investigations are expected to complete the analyses on the even-parity spectra of Pb.

[1] M. J. Seaton, Proc. Phys. Soc. (London) **88**, 801 (1966).
[2] M. J. Seaton, Rep. Prog. Phys. **46**, 167 (1983).
[3] K. T. Lu and U. Fano, Phys. Rev. A **2**, 81 (1970).
[4] U. Fano, Phys. Rev. A **2**, 353 (1970).
[5] K. T. Lu, Phys. Rev. A **4**, 579 (1971).
[6] C. M. Lee and K. T. Lu, Phys. Rev. A **8**, 1241 (1973).
[7] U. Fano, J. Opt. Soc. Am. **65**, 979 (1975).
[8] U. Fano, Phys. Rev. A **17**, 93 (1978). 180 (1977).
[9] U. Feldman, C. M. Brown, G. A. Doschek, C. E. Moore, and F. D. Rosenberg, J. Opt. Soc. Am. **66**, 853 (1976).
[10] C. M. Brown, S. G. Tilford, R. Tousey, and M. L. Ginter, J. Opt. Soc. Am. **64**, 1665 (1974).
[11] C. M. Brown, S. G. Tilford, and M. L. Ginter, J. Opt. Soc. Am. **67**, 584 (1977).
[12] C. M. Brown, S. G. Tilford, and M. L. Ginter, J. Opt. Soc. Am. **67**, 607 (1977).
[13] C. M. Brown, S. G. Tilford, and M. L. Ginter, J. Opt. Soc. Am. **67**, 1240 (1977).
[14] C. E. Moore, *Atomic Energy Levels*, Natl. Bur. Stand. (U.S.) Circ. No. 467 (U.S. GPO, Washington, DC, 1958), Vol. 3.
[15] W. R. S. Garton and M. Wilson, Proc. Phys. Soc. (London), **87**, 841 (1966).
[16] D. R. Wood and K. L. Andrew, J. Opt. Soc. Am. **58**, 818 (1968).
[17] W. A. Young, M. Y. Mirza, and W. W. Duley, J. Phys. B **13**, 3175 (1980).
[18] D. Ding, M. Jin, H. Liu, and X. Liu, J. Phys. B **22**, 1979 (1989).
[19] W. Y. Ma, Q. Hui, L. Q. Li, W. Z. Zhao, K. L. Wen, and D. Y. Chen, in *Resonance Ionization Spectroscopy 1992*, edited by C. M. Miller and J. E. Parks (Institute of Physics, Bristol, 1992), p. 75.
[20] L. J. Moore, J. D. Fassett, and J. C. Travis, Anal. Chem. **56**, 2770 (1984).
[21] B. L. Fearey, C. M. Miller, M. W. Rowe, J. E. Anderson, and N. S. Nogar, Anal. Chem. **60**, 1786 (1988).
[22] E. B. Saloman and W. Happer, Phys. Rev. **144**, 7 (1966).
[23] F. A. Moscatelli, O. Resi, P. Schönberger, H. H. Stroke, and R. L. Wiggins, J. Opt. Soc. Am. **72**, 918 (1982).
[24] R. C. Thompson, M. Anselment, K. Bekk, S. Göring, A. Hanser, G. Meisel, H. Rebel, G. Schantz, and B. A. Brown, J. Phys. G **9**, 443 (1983).
[25] E. B. Saloman, Spectrochim. Act. **45B**, 37 (1990).
[26] F. M. Phelps, *M.I.T. Wavelength Tables* (MIT Press, Cambridge, MA, 1982), Vol. 2.
[27] W. C. Wiley and I. H. McLaren, Rev. Sci. Instrum. **26**, 1150 (1955).